

Zero-Shot Stitching in Reinforcement Learning using Relative Representations

Antonio Pio Ricciardi¹, Valentino Maiorca^{1,2}, Luca Moschella^{1,2}, Riccardo Marin^{3,4}, and Emanuele Rodolà¹

¹Sapienza, University of Rome

²Institute of Science and Technology Austria

³University of Tübingen

⁴Tübingen AI Center

{ricciardi, maiorca, moschella, rodola}@di.uniroma1.it
riccardo.marin@uni-tuebingen.de

Abstract

Visual Reinforcement Learning is a popular and powerful framework that takes full advantage of the Deep Learning breakthrough. However, it is also known that variations in the input (e.g., different colors of the panorama due to the season of the year) or the task (e.g., changing the speed limit for a car to respect) could require complete retraining of the agents. In this work, we leverage recent developments in unifying latent representations to demonstrate that it is possible to combine the components of an agent, rather than retrain it from scratch. We build upon the recent relative representations framework and adapt it for Visual RL. This allows us to create completely new agents capable of handling environment-task combinations never seen during training. Our work paves the road toward a more accessible and flexible use of reinforcement learning.

1 Introduction

Reinforcement Learning (RL) is an effective framework in the field of artificial intelligence to solve sequential decision-making tasks, where agents learn to improve their performance through trial and error (Sutton & Barto, 1998). With the use of Deep Learning, agents are able to act in complex environments and perform complex tasks, such as as robotics control (Levine et al., 2016; 2018) and game playing (Bellemare et al., 2013). Visual RL enables learning complex behaviors directly from images, with solid success (Mnih et al., 2015; Kalashnikov et al., 2018). Despite such progress, RL agents trained end-to-end in the high-dimensional space (such as pixels) suffer from overfitting (Song et al., 2019), which makes it difficult to generalize to unseen scenarios (Cobbe et al., 2019; Lee et al., 2020) and consequently limits real-world applications. Even small changes in the environment could require learning new agents from scratch. This can be expensive, especially for more complex environments. For instance, a self-driving car trained with reinforcement learning in the spring may not operate correctly in the summer if there is a change in the surrounding foliage, despite the track conditions staying the same. When faced with various visual changes and tasks, training a new agent for each scenario is common practice, although this approach is hardly practical.

Previous work proposed different solutions to this problem. Since visual agents rely on encoders to extract relevant features to improve generalization (Shorten & Khoshgoftaar, 2019), methods to augment visual data have been employed (Raileanu et al., 2021; Yarats et al., 2020; Laskin et al., 2020b;a). These methods augment observations of the training environment to help agents ignore task-irrelevant features. This, however, might decrease sample efficiency and make the optimiza-

tion more challenging (Yuan et al., 2022). Indeed, finding the right balance between stability and generalization in RL requires substantial trial and error (Hansen et al., 2021); this process often requires an understanding of the perceptual changes that occur during deployment to ensure proper functioning, as well as significant computational resources causing long training times. Other methods work to produce feature invariance by training encoders to ignore task-irrelevant features Zhang et al. (2020) or by finetuning encoders at deployment to match the latent distribution that was found during training (Hansen et al., 2020; Yoneda et al., 2021). However, these methods assume that deployment tasks do not change from the training ones. Other methods aim to make neural components reusable, allowing model composition, either by imposing training constraints (Devin et al., 2017), using representation learning techniques for low dimensional state space (Jian et al., 2023), or employing relative representations (Moschella et al., 2023) to enable zero or few-shot model stitching.

Inspired by Jian et al. (2023), we leverage the relative representations framework (Moschella et al., 2023) to perform zero-shot stitching between encoders and controllers in the context of Visual RL, where agents receive images as input. We enable the stitching between visual and task variations trained under different conditions. For example, we could reuse the modules of an agent trained to respect a speed limit (controller) during fall (encoder) to maintain the same speed during summer. This is accomplished by connecting its controller with the encoder of another agent trained during summer but with different speed limits. An example of this process can be seen in Figure 1. In the experiment section, we first demonstrate that relative representations have no significant impact in training performance, then perform latent space analysis to evaluate the similarities in the latent spaces among models that use such technique. Finally, we test model performance by conducting experiments in the CarRacing environment (Klimov, 2016), which we modified to explore both visual and task changes, and the Atari suite from Zhang et al. (2018), which allowed us to focus on visual changes. Our experiments demonstrate that encoders and controllers from different models can be combined zero-shot to create new agents, retaining the performance of their original models most of the time, *even when the visual-task combinations have never been seen together at training time*.

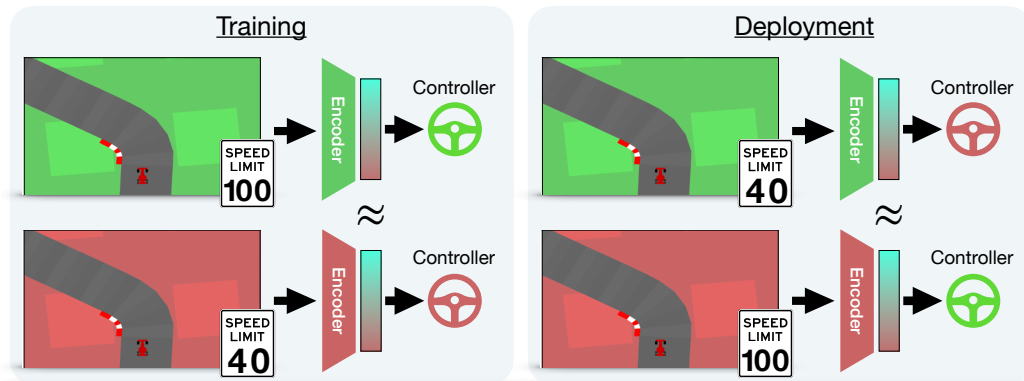


Figure 1: **Training:** We train models end-to-end using relative representations for the encoder output. This ensures that different encoders, trained on various input variations, generate identical outputs when presented with images that only differ in task-irrelevant details. **Testing:** We perform *zero-shot* stitching, connecting the controller module to different encoders it was not trained with. This allows the model to handle new combinations of tasks and environments it never encountered during training.

2 Related works

Model stitching Model stitching refers to the idea of combining different neural networks to create a novel model. It involves integrating parts from multiple networks or ensuring compatibility between latent spaces for tasks such as verifying similarity. Several studies have explored this concept

and introduced techniques to facilitate model stitching. One approach, previously introduced in literature (Lenc & Vedaldi, 2015; Bansal et al., 2021; Csiszarik et al., 2021), uses trainable stitching layers between the source and the target components. Alternatively, certain works have proposed methods that directly generate compatible and reusable network components without relying on explicit stitching layers (Gygli et al., 2021; Yaman et al., 2022). An important concept in this field is that of relative representation (Moschella et al., 2023). Relative representations enable zero-shot stitching between distinct neural networks trained on semantically similar datasets (Norelli et al., 2022). They can be seen as a non-parametric transformation that infuse invariances into the latent spaces to which they are applied. The authors then show that, in many cases, the necessary invariances are for transformations that preserve angles, and they leverage this finding to stitch together different networks trained on semantically similar data.

Invariance and alignment of latent spaces in RL Having agents that adapt to different tasks or visual distractors is a desideratum in RL. Zhang et al. (2020) focus on learning invariant representations for RL using bisimulation metric (Ferns & Precup, 2014) to quantify behavioral similarity between states and learning to disregard task-irrelevant information. Ingebrand et al. (2024) introduce function encoder, a representation learning algorithm which represents a function as a weighted combination of learned, non-linear basis functions to perform zero-shot transfer of policies to similar tasks. The function encoder is trained in a supervised fashion to represent the reward function or the transition function, and is used as an additional input to provide task information to the policy. Other methods perform policy adaption at deployment time to adapt the encoder of the agents to unseen changes in the environment (Hansen et al., 2020; Yoneda et al., 2021). To do so, the first method needs an extra supervised loss during both training and deployment, whereas the second adjusts unsupervisedly at deployment to align the encoder’s output with the training’s latent feature distribution. Nonetheless, both approaches assume the task remains constant, merely accounting for variations in visual observations. Devin et al. (2017) conceptualize policies as combinations of task- and robot-specific modules for zero-shot transfer via novel module pairings. They train flexible modules for mix-and-match capabilities, enabling zero-shot generalization across new robot-task pairs. This process requires initially training controllers with inputs from various environments, then using these controllers to supervise a global neural network policy training through standard supervised learning. They employ regularization to ensure task-invariance and prevent overfitting, restricting agents to a minimal number of hidden units. Jian et al. (2023) introduces *Policy Stitching*, a modular policy framework for transfer learning in robotics, showcasing zero-shot and few-shot transfer abilities in control tasks through relative representations (Moschella et al., 2023). However, it is limited to low-dimensional state representations and relies on model finetuning for latent feature invariance, suggesting the need for alternative module alignment methods beyond anchor states.

Relative Representations Relative representations, as proposed by Moschella et al. (2023), offer a simplified framework for facilitating communication among diverse latent spaces in neural models. This approach introduces an alternative perspective by shifting from an absolute coordinate system to a relative one, with respect to a predefined set of *anchor* samples. Each sample is represented by the distances (or similarities) between its embedding and each of the anchor embeddings. Employing relative representations in a latent space highlights its inherent structure. Under the assumption that good models learn similar representations it enables the latent communication between seemingly dissimilar spaces due to confounding factors.

In this work we leverage on relative representations, similarly to Jian et al. (2023). However, instead of low-dimensional features, we work with rgb images using CarRacing and a subset of the Atari game suite as benchmarks. We train agents using relative representations to allow models encoders to project their latent features into a new space. We show that this space is similar for different visual variations in the same environment. Having a "common" space enables compositionality between encoders and controllers, since controllers are able to interpret the latent space of other encoders, if this space is the same. Similarly to Cannistraci et al. (2023) we analyze the latent space to visualize latent similarity when varying backgrounds. Finally, we show the performance of zero-shot

stitching between encoders and controllers that are trained using relative representations to create new policies for environment visual-task combinations that were never seen together during training.

3 Method

Context. We formally model an RL problem as a Markov decision process (MDP) $\mathcal{M} = (\mathcal{S}, \mathcal{A}, \mathcal{O}, R, P, \gamma)$, where \mathcal{S} defines the set of states, \mathcal{A} the set of actions, $o \in \mathcal{O}$ the observation produced as input for the agents, $P : \mathcal{S} \times \mathcal{A} \mapsto \mathcal{S}$ the probability distribution $P(s'|s, \mathbf{a})$ of transitioning to state s' upon executing action \mathbf{a} in state s , $\mathcal{R} : \mathcal{S} \times \mathcal{A} \mapsto \mathcal{R}$ the reward function, and γ the discount factor that reduces the importance of rewards obtained far in the future. The agent’s behavior is dictated by a policy $\pi : \mathcal{O} \rightarrow \mathcal{A}$ that receives an observation and selects an action at each state, and is trained to maximize the discounted long-term returns $\mathbb{E}[\sum_{i=0}^{\infty} \gamma^i \mathcal{R}(s_i, \mathbf{a}_i)]$.

Environments Variations. To take into account the concept of “variation”, we redefine the environments as follows. First, we will refer to $\mathcal{M}_u^i = (\mathcal{O}_u, T_i)$ as the environment that produces observations $o_u \in \mathcal{O}_u$ and has a task $T_i : \mathcal{S}_i \times \mathcal{A}_i \times \mathcal{R}_i \times P_i \mapsto \mathcal{R}_i$ to solve. We will say that a distribution of observation \mathcal{O}_u is different from another when there is a major variation between them (e.g., background color, camera perspective). At the same time, task variations can impact the agent behavior, and can depend on transition dynamics, internal states, action spaces, and reward functions. Information about the task T_i is not explicitly given to the agent, and it must be inferred using the guidance of the reward signal provided while acting in the environment. During training, we train agents on different combinations of visual-task variations, separately for each combination. When testing, we use environments with visual-task variations never seen during training, i.e., testing on \mathcal{M}_u^i means that no agent has been trained end-to-end to solve the task i for the observations u .

Modular Agents. The standard practice to obtain a policy π_u^i is to end-to-end train a neural network on environment \mathcal{M}_u^i . However, we argue that this network can be seen as a composition of two functions: an encoder $\phi_u^i : \mathcal{O}_u \mapsto \mathcal{X}_u^i$ trained on an environment with an observation space \mathcal{O}_u to produce a latent representation \mathbf{x}_u^i , and a controller $\psi_u^i : \mathcal{X}_u^i \mapsto \mathcal{A}_i$ trained to act on task T_i given the latent representation coming from the encoder. Given an observation o_u , π_u^i can be defined by composition:

$$\pi_u^i(o_u) = \psi_u^i[\phi_u^i(o_u)] = \psi_u^i(\mathbf{x}_u^i). \quad (1)$$

Latent representation. Consider the existence of a second environment $\mathcal{M}_v^j = (\mathcal{O}_v, T_j)$, where the observations \mathcal{O}_v differ from the ones from \mathcal{O}_u just for a visual variation (e.g., different background colors in an Atari game), and a trained policy π_v^j . Given two corresponding observations o_u and o_v (i.e., two observations can be considered identical up to the mentioned variation), it is expected for the latent representations produced by the respective encoders to be different:

$$\phi_u^i(o_u) \neq \phi_v^j(o_v) \quad \text{and therefore} \quad \mathbf{x}_u^i \neq \mathbf{x}_v^j. \quad (2)$$

In the following, we show how to remove this limitation and highlight similarities in the latent representations learned by agents trained in different settings. We formalize our intuition in Section 3.1.

3.1 Relative Representations

The main idea of Relative Representations (Moschella et al., 2023) is to represent latent space elements not in terms of absolute coordinates, but encoding them w.r.t. to some selected samples \mathbf{A} called *anchors*. Namely, given an observation o_u and its corresponding latent space produced by the encoder, $\phi_u^i(o_u) = \mathbf{x}_u^i$, the *relative representations* \mathbf{z}_u^i are produced by computing the similarity

between the encoded frame and the selected anchors:

$$\mathbf{z}_u^i = \text{sim}(\phi_u^i(o_u), \phi_u^i(\mathbf{A}_u)) \quad (3)$$

$$= \text{sim}(\mathbf{x}_u^i, \phi_u^i(\mathbf{A}_u)) \quad (4)$$

$$= [\text{sim}(\mathbf{x}_u^i, \phi_u^i(\mathbf{A}_u^{(0)})), \text{sim}(\mathbf{x}_u^i, \phi_u^i(\mathbf{A}_u^{(1)})), \dots, \text{sim}(\mathbf{x}_u^i, \phi_u^i(\mathbf{A}_u^{(d)}))], \quad (5)$$

where d is the dimension of the latent space and one of the controller’s inputs. Per the original paper, we select the cosine similarity as sim function. However, the original anchor selection process assumes the availability of an offline dataset to sample \mathbf{A} from. Since we are in an online RL setting, we’ll later discuss our data collection strategy to obtain \mathbf{A} .

Intuition. This relative representation disregards the latent points’ absolute positions, which are heavily influenced by the agent’s random initialization, and instead focuses on the relationships between observations. We expect encoders to generate varied absolute latent representations due to visual differences, yet yield *roughly similar relative latent representations*:

$$\text{sim}(\phi_u^i(o_u), \phi_u^i(\mathbf{A}_u)) \approx \text{sim}(\phi_v^j(o_v), \phi_v^j(\mathbf{A}_v)) \quad (6)$$

$$\text{sim}(\mathbf{x}_u^i, \phi_u^i(\mathbf{A}_u)) \approx \text{sim}(\mathbf{x}_v^j, \phi_v^j(\mathbf{A}_v)) \quad (7)$$

$$\mathbf{z}_u^i \approx \mathbf{z}_v^j \quad (8)$$

Thus, we *train the controller directly on the relative spaces* to produce an universal controller, reusable across a variety of settings.

Module stitching. We exploit such quasi-equivalence between the latent relative representation of different agents to perform zero-shot stitching. For example, if we are given policies π_u^i and π_v^j trained with relative representations to act on $\mathcal{M}_u^i = (\mathcal{O}_u, \mathcal{T}_i)$ and $\mathcal{M}_v^j = (\mathcal{O}_v, \mathcal{T}_j)$ respectively, we can combine the encoder ϕ_u^i from π_u^i and the controller ψ_v^j from π_v^j to create a new policy $\hat{\pi}_u^j$ that can act on $\mathcal{M}_u^j = (\mathcal{O}_u, \mathcal{T}_j)$:

$$\hat{\pi}_u^j(o_u) = \psi_v^j(\mathbf{z}_u^i). \quad (9)$$

This can be done because encoders ϕ_u^i and ϕ_v^j produce similar latent spaces, therefore controllers ψ_u^i and ψ_v^j are trained on similar representations. Throughout this paper, we will use encoders and policies trained using PPO.

3.2 Data collection for RL

A key aspect of the relative representations is the selection of a parallel anchor set \mathbf{A} . [Moschella et al. \(2023\)](#) works in a supervised setting where the datasets are given, and anchors can be easily sampled. In RL, datasets typically originate from agent interaction with the environment and are not fixed or integrated into the framework. In [Jian et al. \(2023\)](#), the authors generate a dataset by deploying two policies in their respective environments and use clustering to identify a set of d anchor observations nearest to the cluster centroids, where d represents the latent representation’s dimensionality. A notable limitation of this method is that incorporating new variations requires redefining the anchors and retraining all models with an updated dataset. Our method also collects datasets through policy rollouts but creates separate datasets for each visual variation, with each model trained on its specific variation and anchors. This allows for training new agents on new variations while ensuring they remain compatible with previously trained agents.

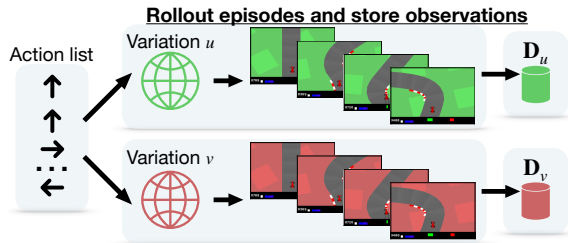


Figure 2: A visualization of the anchors sampling strategy. We perform the same sequence of actions to collect aligned frames from environments with different visual variations, and we use them to build the aligned anchors in the two latent representations.

Anchor sampling. We assume to have access to deterministic environments, i.e., once we fix a seed, this determines the starting state and produces the same transitions given the same sequence of actions. Now suppose we want to collect datasets \mathbf{D}_u and \mathbf{D}_v for environments \mathcal{M}_u^* and \mathcal{M}_v^* . Task is not specified as we are only interested in visual variations to create our datasets. We use a trained policy in \mathcal{M}_u^* and save the sequence of actions \mathbf{a} for several episodes. Then, we use \mathbf{a} to collect observations from both \mathcal{M}_u^* and \mathcal{M}_v^* and form datasets \mathbf{D}_u and \mathbf{D}_v , as seen in Figure 2. Finally, we randomly sample d elements, in parallel, from both datasets to form the anchor sets \mathbf{A}_u and \mathbf{A}_v . These sets are semantically aligned, containing the same interactions with different visual changes.

4 Experiments

In this Section, we assess zero-shot stitched policy performance in previously unseen visual-task combinations within image-based RL. In Section 4.2, we compare the training dynamics of policies that employ relative representations and those that do not (‘absolute’ models). In Section 4.3, we study the latent space similarity to provide a qualitative analysis of the projected spaces, showing that aligned frames with different visual variations exhibit similar latent representations. Finally, in Section 4.4, we report the quantitative performance of Zero-Shot Stitching. Additionally, in the Appendix we show the same tests on a subset of games from the Atari suite.

4.1 Experimental Setup

This section outlines our experimental framework, including notation, how we give decoders context beyond a single image through relative representations, and the tested environments.

Notation. We refer to policies trained *end-to-end* using relative representations as *E. Rel*, and their counterparts using absolute representations as *E. Abs*. In end-to-end models, encoder and controller are trained together simultaneously as a single cohesive unit. Likewise, *S. Abs* denotes models *stitched* with absolute representations, and *S. Rel* refers to those stitched with relative representations. Unlike end-to-end models, stitched agent modules come from encoders and controllers trained independently from each other and connected as detailed in Section 3.1.

Observation context. To make informed predictions, a controller often needs more context than a single image. For example, understanding a ball’s trajectory in Pong requires observing at least two frames. Hence, the choice of anchors for our relative representations must be adapted to deal with frame stacks, as opposed to single images. A simple and effective solution is to decompose the stack, calculate relative representations for each frame, and recombine them back into a stack, giving the controller the needed observation context.

Environments. In the following experiments, we consider the CarRacing (Klimov, 2016) environment, while we refer to Appendix A for experiments on the Atari game suite. Car Racing simulates driving a car from a 2D top-down perspective around a randomly generated track, focusing on speed while staying on the track. It provides RGB image observations, and uses a discretized action space with five options: steer left, steer right, accelerate, brake, and idle. The agent earns rewards for progress and penalties for going off-track. We modified the environment to enable visual changes (e.g. grass color or camera zoom) and task alterations (e.g., speed limits or scrambled action space).

4.2 Training

We train policies using the PPO implementation provided in the CleanRL library (Huang et al., 2022) with default hyperparameters for both absolute and relative representations. Training curves for CarRacing variations are shown in Figure 3. The curves compare *E. Abs.* to *E. Rel.* (**ours**)

under different conditions and are computed using the evaluation scores obtained during training, averaged over four different seeds, with solid lines showing the mean value and the shaded areas the standard deviation. As the figures show, training with relative representations is entirely comparable to standard training.

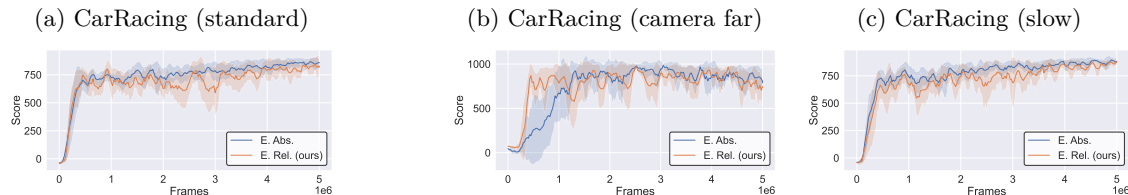


Figure 3: Comparison of E. Abs and E. Rel. training curves. We report three different Car Racing environment variations, noting that in all the training the convergence follows similar tendencies for the two methods and that the relative encoding is not cause of training instability.

4.3 Latent space analysis

We analyzed the latent spaces comparing the features produced by the encoders trained in the CarRacing environment for different grass colors. Similarly to the dataset collection procedure, to collect environment observations, we roll out a policy on an environment and collect the sequence of actions used to act in the environment, setting a fixed seed to ensure reproducibility. We then use the same sequence of actions to collect observations for an episode for two different colors. We compare the similarity between the latent spaces produced by the encoders for the first ~ 800 frames in the episode. Therefore, the diagonal shows the similarity between two perfectly aligned frames where the only difference is the grass color. Figure 4a shows the cosine similarity of the latent space between green and red colors for the absolute and relative spaces, respectively, while Figure 4b shows the frames associated to high similarity points in the relative space. This analysis proves that relative representations enhance latent similarity between semantically similar frames.

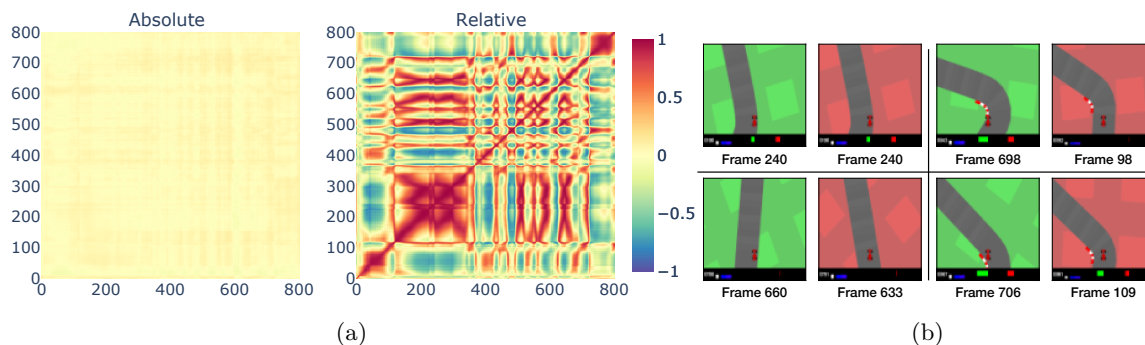


Figure 4: (a) Comparison between absolute (left) and relative (right) representations produced by the same model. Rows and columns show the cosine similarity between the latent spaces coming from frames of the CarRacing environment with different visual variations (i.e., green and red grass color). Relative representations let similarities emerge not only along the diagonal, where frames are aligned, but also off-diagonal, highlighting similarities between different parts of the track. (b) We show a qualitative example by visualizing frame pairs related to high similarity regions in the matrix (denoted by the frame number): the two encode almost the same situation in semantics, showing that relative representations are more suitable in capturing this higher level meaning.

4.4 Evaluating zero-shot stitching

After training different agents on different visual and task variations in the modified Car Racing environment, we froze the encoders and the controllers of each agent and evaluated their zero-shot stitching performance, connecting modules to form a new policy able to play on a specific visual-task variation never-before-seen during training. Encoders and controllers are always chosen according to the visual or task variation they were trained on, respectively. For example, if we are working with a green background, we use an encoder trained on that variation. Similarly, if the task requires driving a car slowly, use a controller trained for that task.

The possible visual variations are: background (grass) colors *green*, *red*, *blue* and *far camera zoom*, while tasks are divided in: *standard* and *slow* car dynamics and different action spaces, such as *scrambled*, which use a different action space and therefore a different output order for the car commands, and *no idle*, which removes the “idle” action. All the tests report the mean scores obtained over ten track seeds, with each seed generating a different track for the agent to drive.

End-to-end performance Before testing the zero-shot stitching performance, we first evaluate how models trained using relative representations compare to standard models in an end-to-end fashion (i.e. without performing stitching). Results in Table 1 show that performance of end-to-end agents trained using relative representations are mostly comparable to those of absolute models, with the exception for the model trained on the slow task.

	Visual variations				Task variations		
	green	red	blue	far (green)	slow	scrambled	no idle
<i>E. Abs</i>	829 ± 54	854 ± 26	852 ± 48	872 ± 35	996 ± 6	879 ± 42	889 ± 19
<i>E. Rel</i> (ours)	832 ± 54	797 ± 86	811 ± 21	820 ± 22	624 ± 125	874 ± 20	862 ± 69

Table 1: Mean scores for models trained end-to-end, without stitching. Models trained using relative representations (*Rel*) have comparable performance, with small performance loss on average. Scores are computed over four training seeds and, for each combination, over ten distinct track seeds.

Zero-shot stitching performance The advantages of relative representations become most apparent in zero-shot stitching, where new agents are formed by combining encoders and controllers from diverse training procedures, including different visual-task variations or training seeds. Models trained with different seeds or under different dynamics, develop different weights, making it impossible to stitch together encoders and controllers. Table 2 shows the performance of zero-shot stitching between encoders and controllers on seed, visual and task variations. Each reported score is the mean calculated across ten seeds for the track, four encoders, and four controllers; each component is trained with a unique seed. Moreover, when **Encoder** and **Controller** variations are the same, we only consider the results obtained for modules trained with different seeds. As the table shows, agents trained using relative representations tend to retain their performance. In contrast, stitching absolute models produces agents that are not able to act in the environment.

5 Conclusion

We show that relative representation can effectively be applied to model reuse in Visual Reinforcement Learning, achieving zero-shot compatibility between neural modules trained with visual and task variations. Further in-depth studies remain to be done, starting from the analysis of the latent space across different algorithms, and an extensive list of visual and task variations to explore how the task and input distribution affect the latent similarities of the learned policies. Moreover, we see value in assessing whether this method could be used to stitch modules across totally different environments having similar semantics at the action level (e.g., different racing games).

		Encoder							
		green		red		blue		far (green)	
		<i>S. Abs</i>	<i>S. Rel</i>	<i>S. Abs</i>	<i>S. Rel</i>	<i>S. Abs</i>	<i>S. Rel</i>	<i>S. Abs</i>	<i>S. Rel</i>
Controller	green	175 ± 304	781 ± 108	157 ± 248	810 ± 52	137 ± 225	791 ± 64	152 ± 204	527 ± 142
	red	167 ± 226	787 ± 62	43 ± 205	776 ± 92	130 ± 274	793 ± 40	65 ± 180	605 ± 118
	blue	-4 ± 79	794 ± 61	22 ± 112	803 ± 58	11 ± 122	805 ± 48	2 ± 152	592 ± 86
	slow	34 ± 178	268 ± 414	73 ± 154	476 ± 430	95 ± 167	564 ± 440	-49 ± 9	303 ± 100
	scrambled	106 ± 217	781 ± 126	138 ± 244	790 ± 72	138 ± 224	804 ± 41	351 ± 97	594 ± 39
	no idle	213 ± 201	824 ± 82	252 ± 228	817 ± 69	144 ± 206	828 ± 50	349 ± 66	673 ± 91

Table 2: Mean score of new agents created via zero-shot stitching, combining encoders and controller trained with different visual-task variations or training seeds. The original domain for the encoders and the controllers is listed in the columns and rows, respectively. Stitching via relative representations greatly outperforms the absolute baseline.

Acknowledgments

This work is supported by the ERC Starting Grant No. 802554 (SPECGEO), PRIN 2020 Project No. 2020TA3K9N (LEGO.AI), PNRR MUR Project PE0000013-FAIR, and by the European Union’s Horizon 2020 research and innovation program under the Marie Skłodowska-Curie grant agreement No 101109330.

References

- Yamini Bansal, Preetum Nakkiran, and Boaz Barak. Revisiting model stitching to compare neural representations. In Marc’Aurelio Ranzato, Alina Beygelzimer, Yann N. Dauphin, Percy Liang, and Jennifer Wortman Vaughan (eds.), *Advances in Neural Information Processing Systems 34: Annual Conference on Neural Information Processing Systems 2021, NeurIPS 2021, December 6-14, 2021, virtual*, pp. 225–236, 2021. URL <https://proceedings.neurips.cc/paper/2021/hash/01ded4259d101feb739b06c399e9cd9c-Abstract.html>.
- Marc G Bellemare, Yavar Naddaf, Joel Veness, and Michael Bowling. The arcade learning environment: An evaluation platform for general agents. *Journal of Artificial Intelligence Research*, 47: 253–279, 2013.
- Irene Cannistraci, Luca Moschella, Marco Fumero, Valentino Maiorca, and Emanuele Rodolà. From bricks to bridges: Product of invariances to enhance latent space communication, 2023.
- Karl Cobbe, Oleg Klimov, Chris Hesse, Taehoon Kim, and John Schulman. Quantifying generalization in reinforcement learning. In Kamalika Chaudhuri and Ruslan Salakhutdinov (eds.), *Proceedings of the 36th International Conference on Machine Learning*, volume 97 of *Proceedings of Machine Learning Research*, pp. 1282–1289. PMLR, 09–15 Jun 2019. URL <https://proceedings.mlr.press/v97/cobbe19a.html>.
- Adrian Csiszarik, Peter Korosi-Szabo, Akos K. Matszangosz, Gergely Papp, and Daniel Varga. Similarity and matching of neural network representations. *ArXiv preprint*, abs/2110.14633, 2021. URL <https://arxiv.org/abs/2110.14633>.
- Coline Devin, Abhishek Gupta, Trevor Darrell, Pieter Abbeel, and Sergey Levine. Learning modular neural network policies for multi-task and multi-robot transfer. In *2017 IEEE international conference on robotics and automation (ICRA)*, pp. 2169–2176. IEEE, 2017.
- Norman Ferns and Doina Precup. Bisimulation metrics are optimal value functions. In *UAI*, pp. 210–219, 2014.
- Michael Gygli, Jasper Uijlings, and Vittorio Ferrari. Towards reusable network components by learning compatible representations. *AAAI*, 35(9):7620–7629, 2021.

-
- Nicklas Hansen, Rishabh Jangir, Yu Sun, Guillem Alenyà, Pieter Abbeel, Alexei A Efros, Lerrel Pinto, and Xiaolong Wang. Self-supervised policy adaptation during deployment. *arXiv preprint arXiv:2007.04309*, 2020.
- Nicklas Hansen, Hao Su, and Xiaolong Wang. Stabilizing deep q-learning with convnets and vision transformers under data augmentation. In *Conference on Neural Information Processing Systems*, 2021.
- Shengyi Huang, Rousslan Fernand Julien Dossa, Chang Ye, Jeff Braga, Dipam Chakraborty, Kinal Mehta, and João G.M. Araújo. Cleanrl: High-quality single-file implementations of deep reinforcement learning algorithms. *Journal of Machine Learning Research*, 23(274):1–18, 2022. URL <http://jmlr.org/papers/v23/21-1342.html>.
- Tyler Ingebrand, Amy Zhang, and Ufuk Topcu. Zero-shot reinforcement learning via function encoders. *arXiv preprint arXiv:2401.17173*, 2024.
- Pingcheng Jian, Easop Lee, Zachary Bell, Michael M Zavlanos, and Boyuan Chen. Policy stitching: Learning transferable robot policies. *arXiv preprint arXiv:2309.13753*, 2023.
- Dmitry Kalashnikov, Alex Irpan, Peter Pastor, Julian Ibarz, Alexander Herzog, Eric Jang, Deirdre Quillen, Ethan Holly, Mrinal Kalakrishnan, Vincent Vanhoucke, et al. Scalable deep reinforcement learning for vision-based robotic manipulation. In *Conference on Robot Learning*, pp. 651–673. PMLR, 2018.
- Oleg Klimov. Carracing-v0. URL <https://gym.openai.com/envs/CarRacing-v0>, 2016.
- Michael Laskin, Aravind Srinivas, and Pieter Abbeel. Curl: Contrastive unsupervised representations for reinforcement learning. In *International Conference on Machine Learning*, pp. 5639–5650. PMLR, 2020a.
- Misha Laskin, Kimin Lee, Adam Stooke, Lerrel Pinto, Pieter Abbeel, and Aravind Srinivas. Reinforcement learning with augmented data. *Advances in neural information processing systems*, 33:19884–19895, 2020b.
- Kimin Lee, Kibok Lee, , Jinwoo Shin, and Honglak Lee. Network randomization: A simple technique for generalization in deep reinforcement learning. In *ICLR*, 2020.
- Karel Lenc and Andrea Vedaldi. Understanding image representations by measuring their equivariance and equivalence. In *IEEE Conference on Computer Vision and Pattern Recognition, CVPR 2015, Boston, MA, USA, June 7-12, 2015*, pp. 991–999. IEEE Computer Society, 2015. doi: 10.1109/CVPR.2015.7298701. URL <https://doi.org/10.1109/CVPR.2015.7298701>.
- Sergey Levine, Chelsea Finn, Trevor Darrell, and Pieter Abbeel. End-to-end training of deep visuomotor policies. *The Journal of Machine Learning Research*, 17(1):1334–1373, 2016.
- Sergey Levine, Peter Pastor, Alex Krizhevsky, Julian Ibarz, and Deirdre Quillen. Learning hand-eye coordination for robotic grasping with deep learning and large-scale data collection. *The International journal of robotics research*, 37(4-5):421–436, 2018.
- Volodymyr Mnih, Koray Kavukcuoglu, David Silver, Andrei A Rusu, Joel Veness, Marc G Bellemare, Alex Graves, Martin Riedmiller, Andreas K Fidjeland, Georg Ostrovski, et al. Human-level control through deep reinforcement learning. *nature*, 518(7540):529–533, 2015.
- Luca Moschella, Valentino Maiorca, Marco Fumero, Antonio Norelli, Francesco Locatello, and Emanuele Rodolà. Relative representations enable zero-shot latent space communication. In *International Conference on Learning Representations*, 2023. URL <https://openreview.net/forum?id=SrC-nwieGJ>.

-
- Antonio Norelli, Marco Fumero, Valentino Maiorca, Luca Moschella, Emanuele Rodolà, and Francesco Locatello. ASIF: Coupled Data Turns Unimodal Models to Multimodal Without Training. *ArXiv preprint*, abs/2210.01738, 2022. URL <https://arxiv.org/abs/2210.01738>.
- Roberta Raileanu, Maxwell Goldstein, Denis Yarats, Ilya Kostrikov, and Rob Fergus. Automatic data augmentation for generalization in reinforcement learning. *Advances in Neural Information Processing Systems*, 34:5402–5415, 2021.
- Connor Shorten and Taghi M Khoshgoftaar. A survey on image data augmentation for deep learning. *Journal of big data*, 6(1):1–48, 2019.
- Xingyou Song, Yiding Jiang, Stephen Tu, Yilun Du, and Behnam Neyshabur. Observational overfitting in reinforcement learning. *arXiv preprint arXiv:1912.02975*, 2019.
- Richard S. Sutton and Andrew G. Barto. *Reinforcement Learning: An Introduction*. The MIT Press, Cambridge, MA, 1998.
- Muammer Y. Yaman, Sergei V. Kalinin, Kathryn N. Guye, David Ginger, and Maxim Ziatdinov. Learning and predicting photonic responses of plasmonic nanoparticle assemblies via dual variational autoencoders. *ArXiv preprint*, abs/2208.03861, 2022. URL <https://arxiv.org/abs/2208.03861>.
- Denis Yarats, Ilya Kostrikov, and Rob Fergus. Image augmentation is all you need: Regularizing deep reinforcement learning from pixels. In *International conference on learning representations*, 2020.
- Takuma Yoneda, Ge Yang, Matthew R Walter, and Bradly Stadie. Invariance through latent alignment. *arXiv preprint arXiv:2112.08526*, 2021.
- Zhecheng Yuan, Guozheng Ma, Yao Mu, Bo Xia, Bo Yuan, Xueqian Wang, Ping Luo, and Huazhe Xu. Don’t touch what matters: Task-aware lipschitz data augmentation for visual reinforcement learning. *arXiv preprint arXiv:2202.09982*, 2022.
- Amy Zhang, Yuxin Wu, and Joelle Pineau. Natural environment benchmarks for reinforcement learning. *arXiv preprint arXiv:1811.06032*, 2018.
- Amy Zhang, Rowan McAllister, Roberto Calandra, Yarín Gal, and Sergey Levine. Learning invariant representations for reinforcement learning without reconstruction. *arXiv preprint arXiv:2006.10742*, 2020.

Appendix

A Atari

To test the generalizability of our method we also perform stitching tests with the following Atari games: Breakout, Boxing, Pong from the NaturalEnv collection (Zhang et al., 2018), which allow background customization with solid colors; the actions are game-specific. In the Breakout environment, scores typically range between 0 and 200-300, representing a satisfactory final score. In Boxing, scores fall within the range of [-100, 100], where a score of 100 indicates that the agent defeats the opponent without sustaining any hits. For Pong, scores range from [-21, 21], with 21 signifying victory over the opponent without conceding a single point. As we did for the CarRacing environment, we first evaluate end-to-end performance of standard and relative models followed by the stitching evaluation.

A.1 Training

The training procedure is the same as described in section 4.2. Training curves comparing E. Abs. to E. Rel. (**ours**) for the Atari suite with visual variations are shown in 5. Also in this case, training using relative representations is comparable to standard training, with the exception of the Breakout environment where the curve tends to grow more slowly.

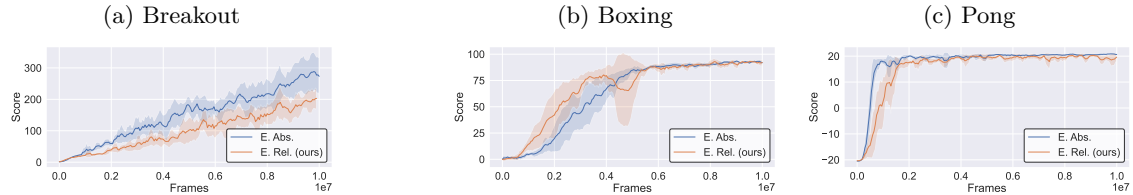


Figure 5: Comparison of E. Abs and E. Rel. training curves for some games in the Atari suite. We see that in all the training the convergence follows similar tendencies for the two methods, and the relative encoding is not cause of training instability.

A.2 Zero-shot stitching

End-to-end performance Results can be seen in Table 3. Performance of relative models for Pong and Boxing are comparable to those of the absolute models. Breakout, however, has much lower scores. We attribute this to the higher visual complexity caused by the numerous bricks in the level.

Zero-shot stitching performance Table 4 presents zero-shot stitching evaluation. Although relative models outperform absolute ones in all the environments, there is a significant performance drop in the mean performance indicated by the lower mean scores. The high the standard deviation, however, signifies that some of the models are still able to perform well in some cases. We argue that the high precision required by Atari games might be the reason for the performance drop in stitching, as even minor mistakes in predictions can result in a losing condition. Meanwhile, the CarRacing environment is far more accommodating, and in the event of a mistake, the policy can compensate in subsequent actions.

		Visual variations		
		plain	green	red
Pong	<i>E. Abs</i>	21 ± 0	21 ± 0	21 ± 0
	<i>E. Rel</i> (ours)	21 ± 0	20 ± 1	21 ± 0
Boxing	<i>E. Abs</i>	95 ± 2	95 ± 3	96 ± 2
	<i>E. Rel</i> (ours)	95 ± 3	93 ± 4	88 ± 6
Breakout	<i>E. Abs</i>	298 ± 63	262 ± 61	132 ± 19
	<i>E. Rel</i> (ours)	146 ± 60	77 ± 25	119 ± 135

Table 3: Episode mean scores for models trained end-to-end, therefore when no stitching is performed. Models trained using relative representations (*Rel*) have comparable performance, with small performance loss on the average.

		Encoder						
		plain		green		red		
		<i>E. Abs</i>	<i>E. Rel</i>	<i>E. Abs</i>	<i>E. Rel</i>	<i>E. Abs</i>	<i>E. Rel</i>	
Controller	Pong	plain	-21 ± 0	0 ± 20	-20 ± 1	-1 ± 20	-21 ± 0	1 ± 18
		green	-21 ± 0	-2 ± 19	-21 ± 0	-7 ± 19	-21 ± 0	-3 ± 18
		red	-21 ± 1	7 ± 17	-21 ± 0	8 ± 18	-21 ± 0	6 ± 20
	Boxing	plain	-29 ± 10	65 ± 39	-18 ± 17	66 ± 38	-27 ± 17	62 ± 40
		green	-25 ± 22	11 ± 54	-21 ± 15	42 ± 36	-20 ± 16	20 ± 56
		red	-33 ± 5	46 ± 40	-33 ± 10	58 ± 27	-38 ± 13	49 ± 39
	Breakout	plain	8 ± 6	71 ± 73	9 ± 7	28 ± 19	9 ± 6	17 ± 9
		green	12 ± 5	16 ± 18	15 ± 4	64 ± 100	13 ± 5	25 ± 28
		red	8 ± 5	17 ± 11	7 ± 6	44 ± 59	8 ± 5	14 ± 10

Table 4: Mean score of new agents created combining encoders and controllers via zero-shot stitching. The original domain for the encoders and the controllers is listed in the columns and rows, respectively. Stitching via relative representations outperforms the absolute approach.